

---

# SSA: SEMANTIC STRUCTURE AWARE INFERENCE FOR WEAKLY PIXEL-WISE DENSE PREDICTIONS WITHOUT COST

---

**Yanpeng Sun**

Nanjing University Of Science And Technology  
Nanjing, Jiangsu, China  
yanpeng\_sun@njjust.edu.cn

**Zechao Li\***

Nanjing University Of Science And Technology  
Nanjing, Jiangsu, China  
zechao.li@njjust.edu.cn

## ABSTRACT

The pixel-wise dense prediction tasks based on weakly supervisions currently use Class Attention Maps (CAM) to generate pseudo masks as ground-truth. However, the existing methods typically depend on the painstaking training modules, which may bring in grinding computational overhead and complex training procedures. In this work, the semantic structure aware inference (SSA) is proposed to explore the semantic structure information hidden in different stages of the CNN-based network to generate high-quality CAM in the model inference. Specifically, the semantic structure modeling module (SSM) is first proposed to generate the class-agnostic semantic correlation representation, where each item denotes the affinity degree between one category of objects and all the others. Then the structured feature representation is explored to polish an immature CAM via the dot product operation. Finally, the polished CAMs from different backbone stages are fused as the output. The proposed method has the advantage of no parameters and does not need to be trained. Therefore, it can be applied to a wide range of weakly-supervised pixel-wise dense prediction tasks. Experimental results on both weakly-supervised object localization and weakly-supervised semantic segmentation tasks demonstrate the effectiveness of the proposed method, which achieves the new state-of-the-art results on these two tasks.

**Keywords** Class Attention Maps · Semantic Structure · Weakly-Supervised object localization · Weakly-Supervised Semantic Segmentation

## 1 Introduction

Class Attention Maps (CAM) serves as an essential technology in a wide range of weakly-supervised pixel-wise dense prediction tasks [1, 2], eg, object location (OL), instance segmentation and semantic segmentation (SS). CAM is proposed to highlight the class-related activation regions for an image classification network, where feature positions related to the specific object class are activated and have higher scores while other regions are suppressed and have lower scores [3]. For specific visual tasks, CAM can be used to infer the object bounding boxes in weakly-supervised OL (WSOL) and generate pseudo-masks of training images in weakly-supervised SS (WSSS). Therefore, obtaining the high-quality CAM is very important to improve the recognition performance of weakly-supervised pixel-wise dense prediction tasks.

Recently, considering that the representation ability of the original CAM (ie, generated by a trained convolutional neural network) is immature and not applicable to complex scenarios, gradient-based methods [4] and erase-based methods [5] are proposed to improve the CAM quality. Specifically, the gradient-based methods [6, 4] obtain CAM by calculating the gradient of the specific image categories relative to deep feature maps. For example, Grad-CAM [4] can extend CAM to various CNN architectures. Although the above methods have achieved satisfied results in some certain scenarios, the gradient-based methods can only capture the most discriminative regions in image, and cannot obtain the detailed features from the image.

The erase-based methods are based on the erasure operation, which improve the localization ability by improving the generalization ability of feature maps [7, 8]. They remove parts from feature maps or images, and then force the learning

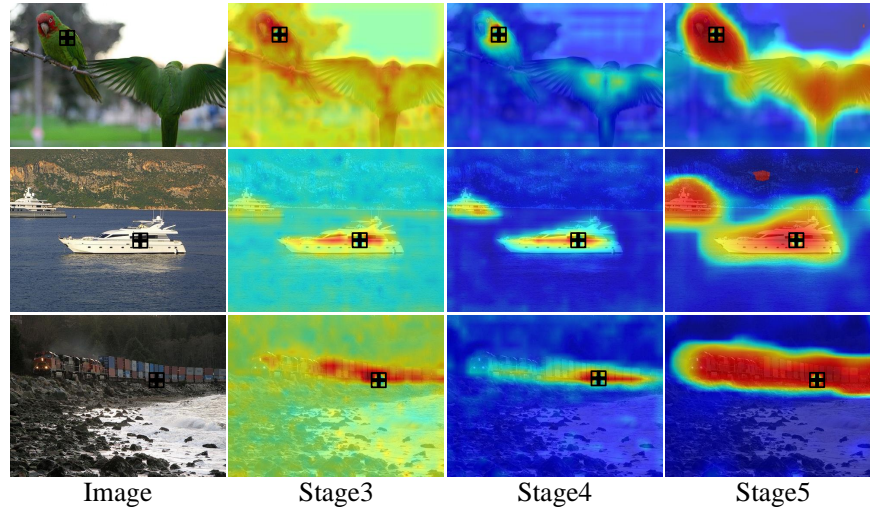


Figure 1: Visualizations of the semantic structure information in backbone stages. The pixels of the same class as the marked pixel are brightly colored. The brighter the color, the higher the similarity. Our motivation comes from this phenomenon.

model to pay more attention to the remaining second-order regions to improve the CAM integrity. For example, Cutout [9] randomly erases rectangular area in the image. However, the erase-based methods often introduce irrelevant regions into the training step and may result in the problem of false positives. In addition, the erased termination conditions are not unique under different datasets, which makes it difficult to generalize to multiple scenarios.

Besides, there are also some common key shortcomings. First, the existing methods are implemented in the model training step, which increases not only the training difficulty of the network, but also the parameters of model. The other common shortcoming is about hyperparameters, because different datasets tend to require different hyperparameters. These shortcomings limit the range of applications of CAM in weakly-supervised tasks. Towards this end, this work aims to design a simple yet efficient method to expand CAM. Rethinking the classification network, to improve the probability of identifying objects, pixels belonging to the same category in the feature map have similar representations. To verify this assumption, as shown in Figure 1, we randomly select one pixel in feature maps generated by different backbone stages to visualize the correlations with other pixels. It can be observed that as the network deepens, the correlation between pixels of the same category in the feature map is stronger. The above visualization results provide strong evidences for our hypothesis and the semantic correlation between pixels is defined as semantic structure information.

Towards this end, this paper proposes a semantic structure aware inference (SSA) model by leveraging different scales of semantic structure information to generate high-quality CAM, and hence improve the recognition performance of downstream tasks. SSA is introduced in the model inference without any training cost. The overall network architecture is shown in Figure 2. Specifically, a seed CAM is first obtained by using the standard image classification network. Then, the semantic structure modeling module (SSM) is proposed and deployed on different backbone stages to generate the semantic relevance representation. After that, the obtained structured feature representations are used to polish the seed CAM via the dot product operation. Finally, the polished CAMs from different backbone stages are fused as the final CAM. To our best knowledge, this is the first work to improve the quality of CAM without parameters in the model inference step. Experimental results on both WSOL and WSSS demonstrate that SSA can achieve new state-of-the-art performance.

The main contributions are summarized as follows:

- This work proposes a novel parameter-free method, termed as semantic structure aware inference (SSA), to improve the CAM quality. It is worth noting that the proposed SSA can be seamlessly integrated into most weakly supervised visual models to improve the performance of the model.
- The semantic structure modeling module is leveraged to extract the semantic structure information hidden in the feature map, and clearly uncover the semantic correlation between pixels.
- SSA achieves the new state-of-the-art performance in WSOL and WSSS.

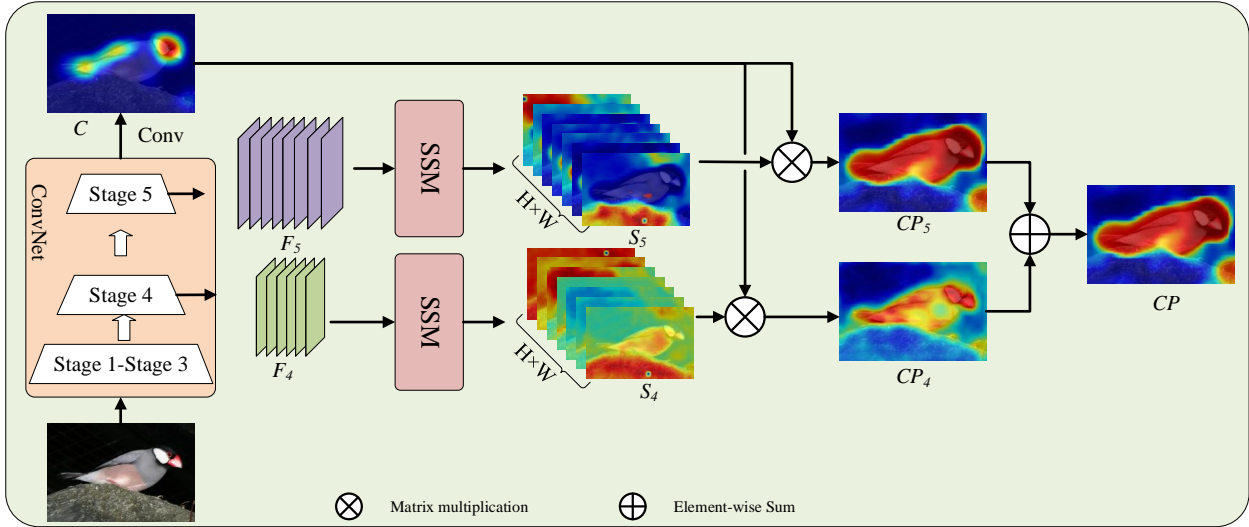


Figure 2: The overall network architecture of the proposed semantic structure aware inference (SSA). Since SSA is only used in the inference CAM stage, it is suitable for all CNN-based models.

## 2 Related Work

### 2.1 The Gradient-based Methods

The gradient-based method [6, 10] generates a class activation maps by combining the back-propagation gradient with the feature map. Among them, the representative Grad-CAM [4] uses training weights derived from the global average gradients to obtain CAM. Based on Grad-CAM, Grad-CAM++ [6] improves the accuracy of object localization by introducing the second-order and the third-order gradients. Besides, XGrad-CAM [10] further introduces two axioms and uses the weighted average gradients to obtain more object details. Smooth Grad-CAM++ [11] introduces gradient smoothing into Grad-CAM++, which improves the ability of visual positioning and class object capture. Group-CAM [12] designs a noise reduction strategy to filter the less important pixels in the initial masks and replace the unreserved area of the mask with the blurry information. The aforementioned methods explore an efficient way to generate CAM. However the CAM obtained by these methods only identify the most discriminative regions of the object. To improve the accuracy of the CAM, the proposed SSA explores the semantic structure information in the network to expand the CAM.

### 2.2 The Erase-based Methods

Recently years, some methods [13, 9] improve the generalization ability of the classification network by erasing part of the image, forcing the classification network to recognize objects through other areas. Starting with the subject of implementation, erase-based methods can be divided into image-level ones and feature-level ones. Image-level methods first erase part of the image, and then force the network to recognize objects through other non-determinative regions. For example, Random Erasing [9] and Cutout [14] randomly erase part of the image. ACoL [2] erases the most discriminative area in the image. AE-PSL [13] erases the area of the CAM from the original image. Feature-level methods dropout units in feature maps during the model training process to prompt the network to focus on other object areas. For example, FickleNet [15] randomly selects hidden feature units during the training phase. ADL [7] uses spatial attention map to hide feature units. These methods not only always require additional computing resources in the training phase, but also introduce many hyper-parameters in the inference phase, which limits their application. Therefore, this paper designs a non-parameter SSA strategy in the inference stage to obtain high-quality CAM without cost.

## 3 Methodology

This section first introduces the process of obtaining seed CAM and the re-discussion of CAM, then elaborates the process of obtaining the semantic structure by SSM, and finally elaborates the detailed process of SSA.

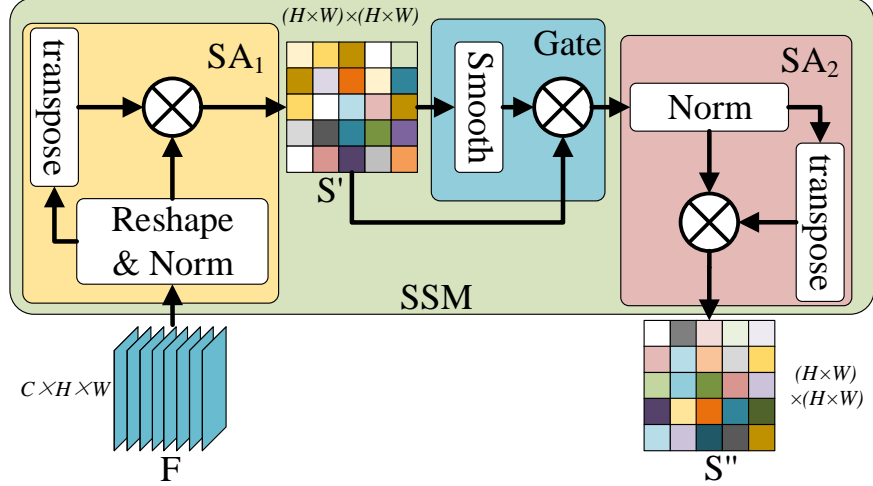


Figure 3: The details of the Semantic Structure modeling Module (SSM)

### 3.1 Rethinking Class Activation Map

The original CAM is based on a convolutional neural network with global average pooling (GAP). In the inference step, the seed CAM is obtained by weighting the feature map of the last convolution layer output with the weights of the last classification layer. Given an image, the seed CAM of ground-truth class  $m$  is computed by:

$$C_m(i, j) = \sum_k \omega_k^m f_k(i, j) \quad (1)$$

where  $(i, j)$  is a coordinate on the feature map  $f$  from the last stage of convolutional neural network,  $\omega$  is the weight of last classification layer and  $k$  is the  $k$ -th channel.

GAP compresses a feature map from the last convolution layer into one-dimensional vector that retains the most important information. The weights of the last classification layer only activate saliency information in the feature map, which makes the seed CAM only focus on the saliency regions in the image. In addition, the structure information of the object is lost in the seed CAM. The semantic structure information can describe the correlation between feature positions, which contains clear category structure features. As shown in Figure 1, there is clear semantic structure information in the trained network. Therefore, it is feasible to explore semantic structure information to expand seed CAM in the inference stage.

### 3.2 SSM Module

Semantic structure information describes the correlation of pixels in the same category, which is very important for polish the semantic structure in CAM. This work proposes the SSM model to extract semantic structure information from the feature maps at different stages. The SSM module is composed of two self-affinity (SA) blocks and a smooth gate, and its structure is shown in the Figure 3.

The feature map  $f$  input to the SSM module can come from different stages of the backbone. To eliminate the adverse effects caused by the singular sample data in feature map  $f$ , we first reshape  $f \in \mathbb{R}^{C \times H \times W}$  to  $\mathbb{R}^{C \times HW}$ , and then normalize it to  $[0, 1]$ :

$$f_{(i,j)} = \frac{f(i, j)}{\sqrt{\sum_{i=1}^H \sum_{j=1}^W f(i, j)}} \quad (2)$$

where  $C$ ,  $H$  and  $W$  represent the channel, width and height of the feature map, respectively. Next, the first SA block captures coarse semantic structure information  $S'$  from the feature map  $f$  by the following equation:

$$S' = f_a^T \cdot f_b - \varepsilon \quad (3)$$

where  $a$  and  $b$  represent the index of features respectively,  $\varepsilon \in \mathbb{R}^{HW \times HW}$  is an identity matrix. To reduce the impact of noise on semantic structure information, SSM introduces a smooth gate. The  $\tanh$  is used to obtain smooth weight

**Algorithm 1** The proposed algorithm SSA

**Input:** Seed CAM  $C \in \mathbb{R}^{N \times H \times W}$ ; Feature maps  $F_4 \in \mathbb{R}^{C_4 \times H \times W}$  and  $F_5 \in \mathbb{R}^{C_5 \times H \times W}$  from Stage 4 and Stage 5, respectively;

**Output:** Final CAM  $CP$

- 1: Using SSM to uncover semantic structure information  $S_4 \in \mathbb{R}^{HW \times HW}$  in  $F_4$ ;
- 2: Reshape  $C$  to  $\mathbb{R}^{N \times HW}$ ;
- 3: Expand  $C$  with  $S_4$  to get  $CP_4 \in \mathbb{R}^{N \times HW}$ ;
- 4: Reshape  $CP_4$  to  $\mathbb{R}^{N \times H \times W}$ ;
- 5: Using SSM to uncover semantic structure information  $S_5 \in \mathbb{R}^{HW \times HW}$  in  $F_5$ ;
- 6: Expand  $C$  with  $S_5$  to get  $CP_5 \in \mathbb{R}^{N \times HW}$ ;
- 7: Reshape  $CP_5$  to  $\mathbb{R}^{N \times H \times W}$ ;
- 8: Fuse  $CP_4$  and  $CP_5$  to get the final CAM  $CP$  by using Eq.8;
- 9: **return**  $CP$

of the coarse semantic structure information  $S'$ . Next, the smooth weight is used to polish  $S'$ :

$$S'_{new} = \tanh(S') \cdot S' \quad (4)$$

It is worth noting that the single SA block cannot completely cover the regions of the object. Thus, SSM leverages the SA block again to further extract more detailed semantic structure information. After the smooth gate, the semantic structure information  $S'_{new} \in \mathbb{R}^{HW \times HW}$  can be regarded as feature map, where the feature representation of each pixel is a  $1 \times HW$  vector. The second SA block first normalizes  $S'_{new}$  to [0,1]:

$$\tilde{S}_{(i,j)} = \frac{S'_{new}(i,j)}{\sum_{i=1}^H \sum_{j=1}^W S'_{new}(i,j)} \quad (5)$$

And then, the second SA block explores relations between  $\tilde{S}_a$  and  $\tilde{S}_b$ :

$$S'' = \phi(\tilde{S}_a^T \cdot \tilde{S}_b - \varepsilon) \quad (6)$$

where  $\phi$  is the function ReLU.  $S''$  is normalized in the same way as Eq. 5. The semantic structure information  $S''$  from the feature map is obtained by the SSM module. The discovered semantic structure information can be regarded as a prior knowledge to guide the process of expanding seed CAM.

### 3.3 Semantic Structure Aware Inference

The seed CAM only focuses on salient regions of object, which loses the structural information of the object. It is worth noting that stage 4 and stage 5 contain clear and different-scale semantic structure information, respectively. To supplement the structural information of objects in the image, SSA extracts different scales semantic structure information from different stages of the backbone to expand seed CAM. Thus, SSA extracts different scales semantic structure information from  $F_4 \in \mathbb{R}^{C_4 \times H \times W}$  and  $F_5 \in \mathbb{R}^{C_5 \times H \times W}$  to expand the seed CAM. First, the seed CAM  $C \in \mathbb{R}^{N \times H \times W}$  is generated from the deep convolutional network, and reshaped to  $\mathbb{R}^{N \times HW}$ . Then SSM is introduced to extract the semantic structure information  $S_4 \in \mathbb{R}^{HW \times HW}$  and  $S_5 \in \mathbb{R}^{HW \times HW}$  from  $F_4$  and  $F_5$ , respectively. Next,  $S_4$  and  $S_5$  are explored to expand seed CAM:

$$CP_4 = \delta(C \odot S_4) \ \& \ CP_5 = \delta(C \odot S_5) \quad (7)$$

where  $\odot$  represents the matrix multiplication and  $\delta$  is a reshape function to reshape the results to  $\mathbb{R}^{N \times H \times W}$ . To further improve the accuracy of CAM, SSA fuses expansion CAM with different scales of semantic structure information to get the final CAM  $CP \in \mathbb{R}^{N \times H \times W}$ :

$$CP = CP_4 \oplus CP_5 \quad (8)$$

where  $\oplus$  represents element-wise sum.

With SSA, the seed CAM integrates different scales of semantic structure information, making the final CAM cover a more comprehensive regions, and clearer object structure features. It is very important for weakly supervised vision tasks.

Table 1: Ablation study based on the number of SA block in SSM module. N-SA denotes the number of the SA block.

Method	N-SA	Error rate (%)		
		TOP-1	TOP-5	GT-known
CAM [3]	-	55.9	47.8	44.0
CAM + SSA	1	45.1	33.2	29.2
CAM + SSA	2	<b>44.9</b>	<b>33.0</b>	<b>29.1</b>
CAM + SSA	3	49.2	38.2	34.2
SPA + SCG [3]	-	40.49	28.4	23.0
SPA + SSA	1	38.6	25.1	19.8
SPA + SSA	2	<b>38.1</b>	<b>24.9</b>	<b>19.4</b>
SPA + SSA	3	41.8	29.8	24.6

## 4 Experiments

This section conducts experiments to evaluate the proposed SSA on two weakly supervised visual tasks: weakly supervised object localization (WSOL) and weakly supervised semantic segmentation (WSSS) with image-level class labels.

**Common Settings.** All experimental systems are based on Pytorch [16]. Both tasks are only annotated with image-level labels for training. All models are pre-trained on ILSVRC [17].

### 4.1 WSOL Settings

**Datasets.** To evaluate the SSA in WSOL task, extensive experiments are conducted on two publicly available benchmarks including CUB-200-2011 [18] and ILSVRC [17]. The CUB-200-2011 is a fine-grained bird dataset with 200 categories, where the training set has 5,994 images and test set has 5,794 images. The ILSVRC consists of 1,000 classes, while has 1.2 million images for the training set and 50,000 images for the validation set. In addition to image-level labels in WSOL task, the bounding box labels are also required. For ILSVRC, SEM [1] provides pixel level annotation of 44,270 images for evaluating IOU curve, which is divided into the validation set (23,150 images) and the test set (21,120 images).

**Training Details and Metrics.** For metrics, we use two kinds of metrics to evaluate bounding box and mask from the CAM. Following the previous works [8, 19], the location performance is measured by TOP1/TOP5 error and known ground-truth class (GT-known). GT-known judges the map as correct when the predicted bounding boxes have over 50% intersection over union (IoU) with the ground-truth boxes. The mask performance is measured by IoU curve following SEM [1]. The IoU curve is obtained by calculating the IoU scores between the foreground pixels and the ground-truth masks under different thresholds. High IoU scores and threshold value indicates high-quality maps. We verify the performance of SSA on VGG16 [20] and Inception V3 [21] network respectively. For data augmentation, the input images are resized to  $256 \times 256$  pixels and randomly cropped to  $224 \times 224$  pixels. For classification, we average the scores from the softmax layer with 10 crops.

### 4.2 WSSS Settings

**Datasets.** To verify the validity of SSA in WSSS, experiments are conducted on the PASCAL VOC 2012 [22] dataset, which contains 1,464 images in the training set, 1,449 images in the validation set and 1,456 images in the test set. Following the common practice, the augmented dataset [23] expands the training set from the original data to 10,582 images, which have image-level labels. This dataset contains pixel-level labels for fully supervised segmentation, but we use the image-level class labels for training and pixel-level labels for evaluation.

**Training Details and Metrics.** To evaluate the performance of weakly semantic segmentation, the widely used mean intersection-over-union (mIoU) is introduced. Following the previous work [24], ResNet50 [25] is used to generate the initial seed, and then IRNet [26] is used to generate the pseudo labels. For fair competition, DeepLab-v2-ResNet101 [27] is used in the final segmentation stage. In the CAM generation phase, to eliminate the noise caused by flip inference, we first use the *HardTanh* function with range  $[0, 1]$  to obtain the significant map  $SM_4$  and  $SM_5$  in  $CP_4$  and  $CP_5$ , then use  $SM_4$  to guide the generation of  $CP_5$ , and  $SM_5$  to guide the generation of  $CP_4$ . The initial learning rate is set to 0.1 with 10 epoch for training classification network, while 5 epoch for training IRNet. In the final segmentation, the batch size is set to 10, and the learning rate is set to  $2.5e-4$  with 30K.



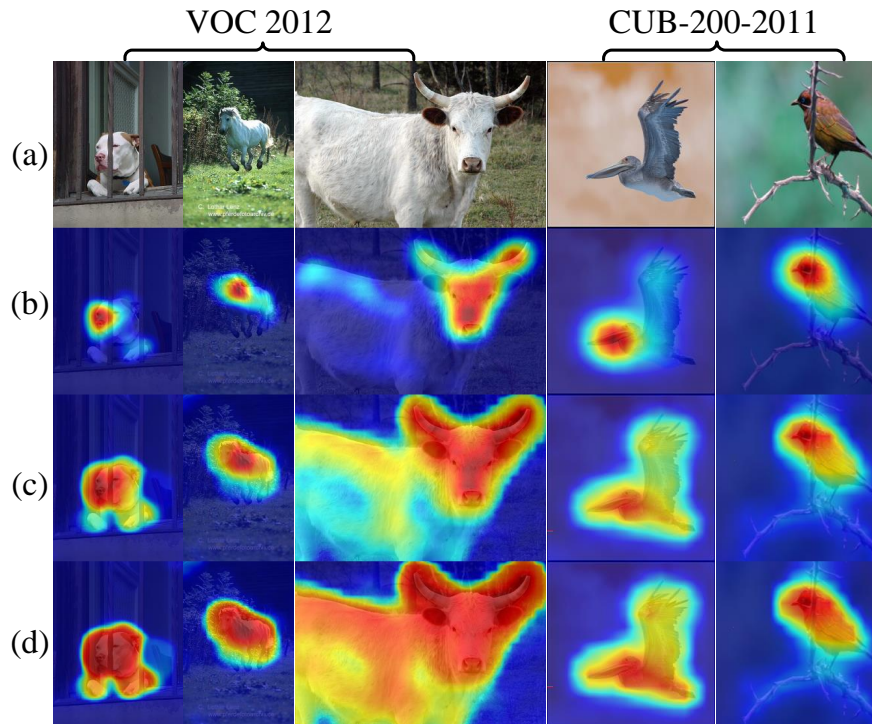


Figure 4: Visualization results of SSA with different numbers of SA-blocks. (a) input image, (b) seed CAM, (c) and (d) are the results of SSA after using SA block once and twice, respectively.

### 4.3 Ablation Study

This section conducts a series of ablation study on the CUB-200-2011, ILSVRC and PASCAL VOC 2012 datasets. The results are obtained by using VGG16 as the backbone on CUB-200-2011 and using ResNet50 as the backbone on PASCAL VOC 2012. VGG16 and Inception V3 are used as the backbone on ILSVRC respectively. We first verify the effectiveness of the proposed SSM module, then verify the strength of the semantic structure information at different stages, and finally verify the universality of SSA.

**For SSM.** In the SSM module, the SA block is proposed to capture the semantic structure in the features. Thus, the ablation study is conducted to show the superiority of the SSM module. First, experiments are conducted to verify the influence of the number of SA blocks (N-SA) in the SSM model. The number of SA is tuned within [1, 2, 3]. Experimental results based on CAM [3] and SPA [19] are shown in Table 1. It can be easily seen that when the SSM module uses two SA blocks, the best performance is achieved, which indicates that the SSM module obtains more detailed semantic structure information from the feature map. To visually observe the influence of N-SA on the final CAM, we performed a visualization experiment. The result are shown in Figure 4. The visualization results show that when N-SA is 2, the regions of the final CAM is more accurate than when the number of SA blocks is 1. For example, in the third column images of Fig.4, when the SA block is used only once, the CAM can only cover the head of the cow. When the SA block is used twice, CAM can cover the whole body of the cow. Experimental results show that SSM can obtain more accurate semantic structure information from the feature map after using two SA blocks.

**For SSA.** The most important part in SSA is to explore the semantic structure information from different stages to expand the seed CAM. Therefore, which stage has more detailed semantic structure information is the focus of the next study. To verify the validity of the semantic structure information in different stages, SSA first uses the SSM module to extract the semantic structure information in different stages, then expands the seed CAM through it, and finally observes its performance in the WSOL task. SPA without SCG [19] serves as the benchmark for this experiment. The ablation study results are presented in Table 2. It can be easily observed that the semantic structure information in stage 5 improves the model performance most. To visually observe the changes of the final CAM that integrates the semantic structure information of different stages, we conducted a visualization experiment, and the results are shown in Figure 5. The results show that stage 3 introduces a lot of noise information for final CAM, and stage 4 introduces noise for final CAM, but it can clearly cover all areas of the object. Although the final CAM obtained using stage 5 covers the largest area, it has the phenomenon of over-recognition. In order to further improve the quality of CAM, a simple method is to

Table 2: Ablation study of SSA on CUB-200-2011. **Stage** indicates the semantic structure information of which stage is used to expand the seed CAM.

Stage	Error rate (%)		
	TOP-1	TOP-5	GT-known
††	49.0	38.5	34.1
Stage 3	66.4	59.2	56.5
Stage 4	44.8	33.0	28.1
Stage 5	<b>40.1</b>	<b>27.3</b>	<b>21.9</b>
Stage 3 + Stage 4	49.7	39.3	34.7
Stage 3 + Stage 5	40.0	27.0	21.6
Stage 4 + Stage 5	<b>38.1</b>	<b>24.9</b>	<b>19.4</b>
Stage 3 + Stage 4 + Stage5	39.0	26.1	20.6

†† denotes the benchmark SPA without SCG

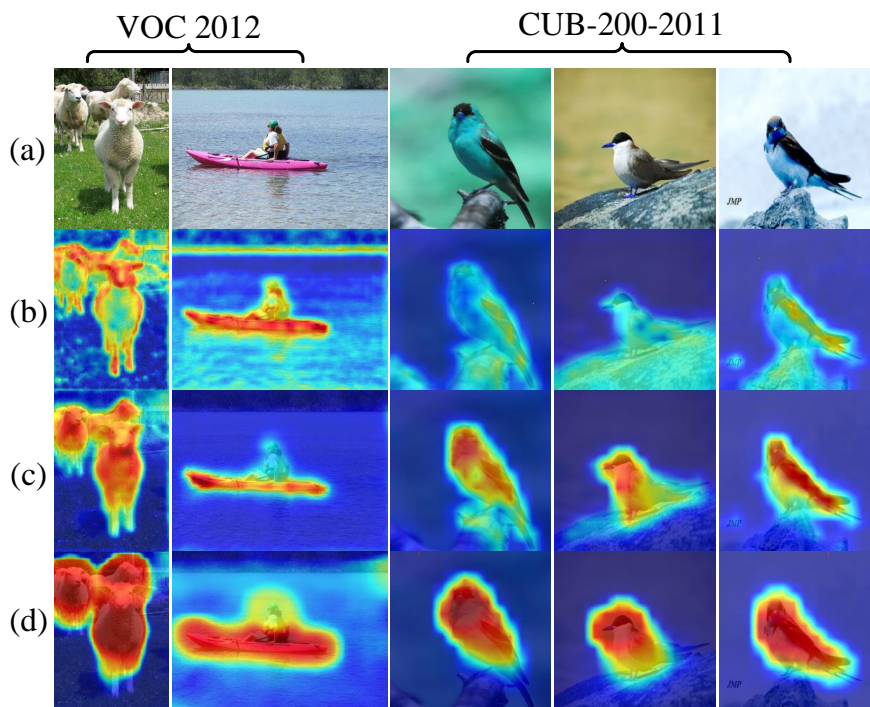
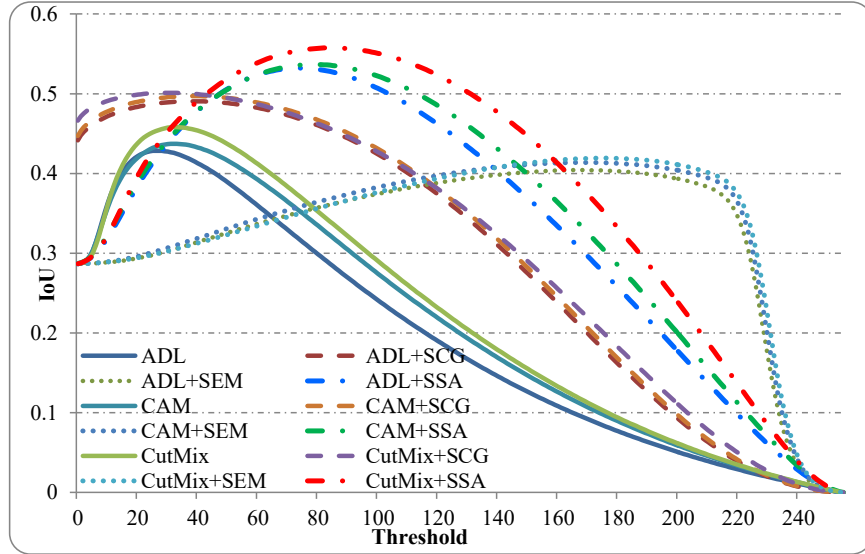


Figure 5: Visualization results of SSA with semantic structure information of different stages. (a) input image, (b) using Stage 3, (c) using Stage 4 and (d) using Stage 5

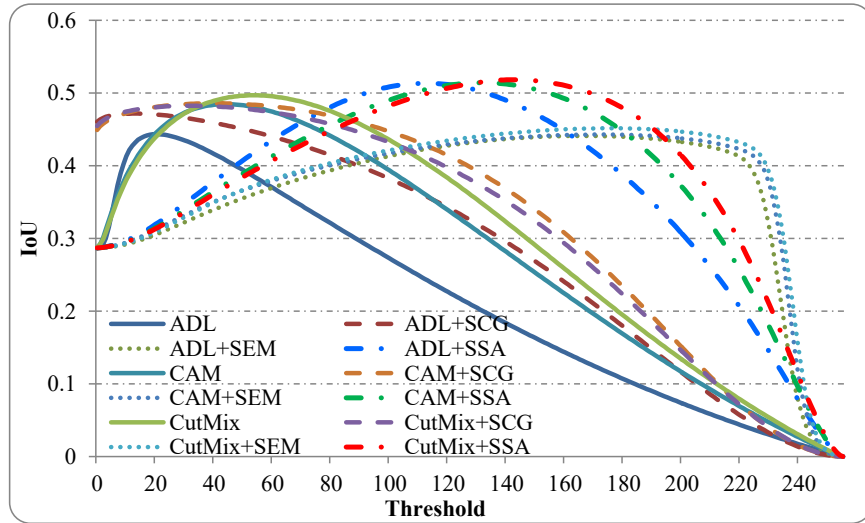
merge the CAM after fusing the semantic structure information of different stages. The results are show in Table 2. It can be seen that the fusion of stage 4 and stage 5 can further improve the performance of SSA. Due to the excessive noise in stage 3, the combination of stage 3 cannot improve the quality of CAM.

**For the universality and superiority of SSA.** To verify the universality of SSA, IoU curve is used to evaluate the performance of SSA on the ILSVRC dataset. The compared methods include ADL [7], CAM [3] and CutMix [28] based on VGG16 and Inception V3. In addition, the superiority of SSA is verified by comparing SSA, SEM [1] and SCG [19], which expand CAM in the inference step. The IoU curve results are shown in Figure 6. It can be seen that SSA greatly improves the quality of CAM, and the change of backbones does not affect the performance of SSA. Experimental results show that although the accuracy of CAM obtained by SCG is improved, the mask generated by CAM has the worst visual effect. The mask obtained by SEM has a good visual effect, but its localization accuracy is very poor. Compared with SCG and SEM, the mask obtained by SSA has not only higher localization accuracy, but also better visual effects. High-quality CAM generated mask is characterized by high clarity and high localization accuracy, which are important for weakly supervised vision tasks. Therefore, in order to further improve the quality of CAM, SSA is the best choice in the inference step.





(a) The IoU curve results based on VGG16



(b) The IoU curve results based on Inception V3

Figure 6: Compared results in terms of IoU curve on the ILSVRC dataset.

#### 4.4 State-of-the-Art Comparisons

**Comparison with SOTA in WSOL.** To verify the effectiveness of the proposed SSA in object localization, experiments are carried out on the CUB-200-2011 and ILSVRC datasets. SSA based on SPA [19] and CAM [3] are compared with SPG [8], DANet [29], SEM [1], I<sup>2</sup>C [30], etc. Table 3 shows the experimental results of SSA and SOTA methods on the CUB-200-2011 test set. By using Inceptionv3 as the backbone, SSA surpasses all the compared methods and achieves TOP1 localization error rate of 44.9% in the original CAM. With VGG16, SSA achieves the TOP1 localization error rate of 44.9% in the original CAM, and TOP1 localization error rate of 38.1% based on the stronger classification network (SPA), which surpasses all the baselines. Table 4 reports the results on the ILSVRC test set. It can be seen that SSA achieves TOP1 localization error rate of 50.7%, surpassing all the baselines. Based on the same network, compared with SCG, SSA reduces the TOP1 localization error rate by 2.4% and 0.4% on the CUB-200-2011 and ILSVRC data sets, respectively. It shows that SSA can be seamlessly integrated into any CNN-based network to improve the quality of CAM, thereby improving the performance of object localization without cost.

**Comparison with SOTA in WSSS.** To verify the effectiveness of SSA in multi-label tasks, we conducted experiments on PASCAL VOC 2012 dataset for the WSSS task. The SSA is applied in the CAM generation step. Following the previous work [24], IRNet is used for post-processing to generate pseudo-labels. Our method is compared with CIAN

Table 3: Comparison with state-of-the-arts on the CUB-200-2011 test set.

Method	Backbone	Error rate (%)		
		TOP-1	TOP-5	GT-known
CAM [3]	GoogLeNet	58.9	49.3	44.9
SPG [8]	GoogLeNet	53.4	42.8	-
CAM [3] †	InceptionV3	53.8	42.8	38.3
DANet [29]	InceptionV3	50.6	39.5	33.0
SEM [1]	GoogLeNet	47.0	-	30.0
ADL [7]	InceptionV3	47.0	-	-
SPA+SCG [19]	InceptionV3	46.4	33.5	27.9
<b>CAM + SSA</b>	<b>InceptionV3</b>	<b>44.9</b>	<b>31.5</b>	<b>25.5</b>
CAM [3]	VGG16	55.9	47.8	44.0
ACoL [2]	VGG16	54.1	43.5	45.9
SPG [8]	VGG16	51.1	42.2	41.1
ADL [7]	VGG16	47.6	-	-
DANet [29]	VGG16	47.5	38.0	32.3
I <sup>2</sup> C [30]	VGG16	44.0	31.6	-
MEIL [31]	VGG16	42.5	-	-
SPA+SCG [19] †	VGG16	40.5	28.4	22.9
<b>CAM + SSA</b>	<b>VGG16</b>	<b>44.9</b>	<b>33.0</b>	<b>29.1</b>
<b>SPA + SSA</b>	<b>VGG16</b>	<b>38.1</b>	<b>24.9</b>	<b>19.4</b>

† denotes the results implemented by us

Table 4: Comparison with state-of-the-arts on the ILSVRC test set.

Method	Backbone	Error rate (%)		
		TOP-1	TOP-5	GT-known
CAM [3]	VGG16	57.2	45.1	-
CutMix [28]	VGG16	56.6	-	-
SEM [1]	VGG16	55.4	-	39.2
ADL [7]	VGG16	55.1	-	-
ACoL [2]	VGG16	54.2	40.6	37.0
MEIL [31]	VGG16	53.2	-	-
I <sup>2</sup> C [30]	VGG16	52.6	41.5	36.1
SPA+SCG [19] †	VGG16	51.1	39.5	35.1
<b>SPA + SSA</b>	<b>VGG16</b>	<b>50.7</b>	<b>39.0</b>	<b>34.4</b>

[32], OAA [33], SEAM [34], CONTA [24] etc. Experiments results are presented in Table 5. It can be observed that SSA achieves the best result 67.4% and 67.9% mIoU on the val and test sets respectively, which surpasses all the baselines. Specifically, the performance of SSA surpasses methods such as BoxSup [35] and SDI [36] that use bounding boxes as supervisory information. In addition, compared with IRNet, SSA improves the performance on the val and test data sets by 3.9% and 3.1% mIoU, respectively. It shows that the proposed SSA can help CAM to cover more correct areas, and obtain high-quality pseudo-labels.

## 5 Conclusion

This paper proposes a new semantic structure aware inference (SSA) for weakly pixel-wise dense predictions, which explores different scales of semantic structure information to generate high-quality CAM in inference. Specifically, The Semantic Structure modeling Module (SSM) is developed to explore the semantic structure on different backbone stages. Then, the semantic structure is leveraged to expand the seed CAM, and finally the expand CAMs on different stages are merged to obtain the final CAM. The proposed SSA can be applied to any CNN-based method to improve the quality of CAM. SSA achieves superior performance on WSOL and WSSS tasks, respectively. However, the generalization ability of semantic structure information is insufficient. Thus how to improve the generalization ability of the semantic structure information is the focus of our future research.

Table 5: Comparison with state-of-the-arts on the PASCAL VOC 2012 val and test sets.

Method	Sup.	val	test
<i>Fully supervised</i>			
FCN [37]	$\mathcal{P}$ .	-	62.2
Deeplab [27]	$\mathcal{P}$ .	67.7	70.3
<i>Weakly supervised</i>			
BoxSup [35]	$\mathcal{B}$ .	62.0	64.6
SDI [36]	$\mathcal{B}$ .	65.7	67.5
MCIS [38]	$\mathcal{I.S.W}$ .	67.7	67.5
OAA++ <sup>+</sup> [39]	$\mathcal{I.S}$ .	66.1	67.2
AttnBN [40]	$\mathcal{I.S}$ .	62.1	63.0
OAA [33]	$\mathcal{I.S}$ .	63.9	65.6
FickeNet [15]	$\mathcal{I.S}$ .	64.9	65.3
MCIS [38]	$\mathcal{I.S}$ .	66.2	66.9
CIAN [32]	$\mathcal{I.S}$ .	64.3	65.3
SEC [41]	$\mathcal{I}$ .	50.7	51.7
AE-PSL [13]	$\mathcal{I}$ .	55.0	55.7
IRNet [26]	$\mathcal{I}$ .	63.5	64.8
SSDD [42]	$\mathcal{I}$ .	64.9	65.5
SEAM [34]	$\mathcal{I}$ .	64.5	65.7
SC-CAM [43]	$\mathcal{I}$ .	66.1	65.9
CONTA [24]	$\mathcal{I}$ .	66.1	66.7
IRNet + SSA	$\mathcal{I}$ .	<b>67.4</b>	<b>67.9</b>

$\mathcal{P}$ .-Pixel level mask,  $\mathcal{B}$ .-Box,  $\mathcal{I}$ .-Image level class,  $\mathcal{W}$ .-Web

## References

- [1] Xiaolin Zhang, Yunchao Wei, Yi Yang, and Fei Wu. Rethinking localization map: Towards accurate object perception with self-enhancement maps. *arXiv*, 2020.
- [2] Xiaolin Zhang, Yunchao Wei, Jiashi Feng, Yi Yang, and Thomas S Huang. Adversarial complementary learning for weakly supervised object localization. In *Proceedings of the IEEE Conference on Computer Vision and Pattern Recognition*, pages 1325–1334, 2018.
- [3] Bolei Zhou, Aditya Khosla, Agata Lapedriza, Aude Oliva, and Antonio Torralba. Learning deep features for discriminative localization. In *Proceedings of the IEEE Conference on Computer Vision and Pattern Recognition*, pages 2921–2929, 2016.
- [4] Ramprasaath R Selvaraju, Michael Cogswell, Abhishek Das, Ramakrishna Vedantam, Devi Parikh, and Dhruv Batra. Grad-cam: Visual explanations from deep networks via gradient-based localization. In *Proceedings of the IEEE International Conference on Computer Vision*, pages 618–626, 2017.
- [5] Haofan Wang, Rakshit Naidu, Joy Michael, and Soumya Snigdha Kundu. Ss-cam: Smoothed score-cam for sharper visual feature localization. *arXiv*, 2020.
- [6] Aditya Chattopadhyay, Anirban Sarkar, Prantik Howlader, and Vineeth N Balasubramanian. Grad-cam++: Generalized gradient-based visual explanations for deep convolutional networks. In *2018 IEEE Winter Conference on Applications of Computer Vision*, pages 839–847. IEEE, 2018.
- [7] Junsuk Choe and Hyunjung Shim. Attention-based dropout layer for weakly supervised object localization. In *Proceedings of the IEEE Conference on Computer Vision and Pattern Recognition*, pages 2219–2228, 2019.
- [8] Xiaolin Zhang, Yunchao Wei, Guoliang Kang, Yi Yang, and Thomas Huang. Self-produced guidance for weakly-supervised object localization. In *Proceedings of the European Conference on Computer Vision*, pages 597–613, 2018.
- [9] Zhun Zhong, Liang Zheng, Guoliang Kang, Shaozi Li, and Yi Yang. Random erasing data augmentation. In *Proceedings of the AAAI Conference on Artificial Intelligence*, pages 13001–13008, 2020.
- [10] Ruigang Fu, Qingyong Hu, Xiaohu Dong, Yulan Guo, Yinghui Gao, and Biao Li. Axiom-based grad-cam: Towards accurate visualization and explanation of cnns. In *British Machine Vision Conference*, 2020.

- [11] Daniel Omeiza, Skyler Speakman, Celia Cintas, and Komminist Weldermariam. Smooth grad-cam++: An enhanced inference level visualization technique for deep convolutional neural network models. *arXiv*, 2019.
- [12] Qinglong Zhang, Lu Rao, and Yubin Yang. Group-cam: Group score-weighted visual explanations for deep convolutional networks. *arXiv*, 2021.
- [13] Yunchao Wei, Jiashi Feng, Xiaodan Liang, Ming-Ming Cheng, Yao Zhao, and Shuicheng Yan. Object region mining with adversarial erasing: A simple classification to semantic segmentation approach. In *Proceedings of the IEEE Conference on Computer Vision and Pattern Recognition*, pages 1568–1576, 2017.
- [14] Terrance DeVries and Graham W Taylor. Improved regularization of convolutional neural networks with cutout. *arXiv*, 2017.
- [15] Jungbeom Lee, Eunji Kim, Sungmin Lee, Jangho Lee, and Sungroh Yoon. Ficklenet: Weakly and semi-supervised semantic image segmentation using stochastic inference. In *Proceedings of the IEEE Conference on Computer Vision and Pattern Recognition*, pages 5267–5276, 2019.
- [16] Adam Paszke, Sam Gross, Francisco Massa, Adam Lerer, James Bradbury, Gregory Chanan, Trevor Killeen, Zeming Lin, Natalia Gimelshein, Luca Antiga, et al. Pytorch: An imperative style, high-performance deep learning library. *Advances in Neural Information Processing Systems*, 32:8026–8037, 2019.
- [17] Olga Russakovsky, Jia Deng, Hao Su, Jonathan Krause, Sanjeev Satheesh, Sean Ma, Zhiheng Huang, Andrej Karpathy, Aditya Khosla, Michael Bernstein, et al. Imagenet large scale visual recognition challenge. *International Journal of Computer Vision*, 115(3):211–252, 2015.
- [18] Catherine Wah, Steve Branson, Peter Welinder, Pietro Perona, and Serge Belongie. The caltech-ucsd birds-200-2011 dataset. 2011.
- [19] Xingjia Pan, Yingguo Gao, Zhiwen Lin, Fan Tang, Weiming Dong, Haolei Yuan, Feiyue Huang, and Changsheng Xu. Unveiling the potential of structure preserving for weakly supervised object localization. In *Proceedings of the IEEE Conference on Computer Vision and Pattern Recognition*, pages 11642–11651, 2021.
- [20] Karen Simonyan and Andrew Zisserman. Very deep convolutional networks for large-scale image recognition. *arXiv*, 2014.
- [21] Christian Szegedy, Vincent Vanhoucke, Sergey Ioffe, Jon Shlens, and Zbigniew Wojna. Rethinking the inception architecture for computer vision. In *Proceedings of the IEEE Conference on Computer Vision and Pattern Recognition*, pages 2818–2826, 2016.
- [22] Mark Everingham, Luc Van Gool, Christopher KI Williams, John Winn, and Andrew Zisserman. The pascal visual object classes (voc) challenge. *International Journal of Computer Vision*, 88(2):303–338, 2010.
- [23] Bharath Hariharan, Pablo Arbeláez, Lubomir Bourdev, Subhransu Maji, and Jitendra Malik. Semantic contours from inverse detectors. In *Proceedings of the IEEE International Conference on Computer Vision*, pages 991–998. IEEE, 2011.
- [24] Dong Zhang, Hanwang Zhang, Jinhui Tang, Xian-Sheng Hua, and Qianru Sun. Causal intervention for weakly-supervised semantic segmentation. *Advances in Neural Information Processing Systems*, 33, 2020.
- [25] Kaiming He, Xiangyu Zhang, Shaoqing Ren, and Jian Sun. Deep residual learning for image recognition. In *Proceedings of the IEEE Conference on Computer Vision and Pattern Recognition*, pages 770–778, 2016.
- [26] Jiwoon Ahn, Sunghyun Cho, and Suha Kwak. Weakly supervised learning of instance segmentation with inter-pixel relations. In *Proceedings of the IEEE Conference on Computer Vision and Pattern Recognition*, pages 2209–2218, 2019.
- [27] Liang-Chieh Chen, George Papandreou, Iasonas Kokkinos, Kevin Murphy, and Alan L Yuille. Deeplab: Semantic image segmentation with deep convolutional nets, atrous convolution, and fully connected crfs. *IEEE Transactions on Pattern Analysis and Machine Intelligence*, 40(4):834–848, 2017.
- [28] Sangdoon Yun, Dongyoon Han, Seong Joon Oh, Sanghyuk Chun, Junsuk Choe, and Youngjoon Yoo. Cutmix: Regularization strategy to train strong classifiers with localizable features. In *Proceedings of the IEEE International Conference on Computer Vision*, pages 6023–6032, 2019.
- [29] Haolan Xue, Chang Liu, Fang Wan, Jianbin Jiao, Xiangyang Ji, and Qixiang Ye. Danet: Divergent activation for weakly supervised object localization. In *Proceedings of the IEEE International Conference on Computer Vision*, pages 6589–6598, 2019.
- [30] Xiaolin Zhang, Yunchao Wei, and Yi Yang. Inter-image communication for weakly supervised localization. In *Proceedings of the European Conference on Computer Vision*, pages 271–287. Springer, 2020.

- [31] Jinjie Mai, Meng Yang, and Wenfeng Luo. Erasing integrated learning: A simple yet effective approach for weakly supervised object localization. In *Proceedings of the IEEE Conference on Computer Vision and Pattern Recognition*, pages 8766–8775, 2020.
- [32] Junsong Fan, Zhaoxiang Zhang, Tieniu Tan, Chunfeng Song, and Jun Xiao. Cian: Cross-image affinity net for weakly supervised semantic segmentation. In *Proceedings of the AAAI Conference on Artificial Intelligence*, pages 10762–10769, 2020.
- [33] Peng-Tao Jiang, Qibin Hou, Yang Cao, Ming-Ming Cheng, Yunchao Wei, and Hong-Kai Xiong. Integral object mining via online attention accumulation. In *Proceedings of the IEEE International Conference on Computer Vision*, pages 2070–2079, 2019.
- [34] Yude Wang, Jie Zhang, Meina Kan, Shiguang Shan, and Xilin Chen. Self-supervised equivariant attention mechanism for weakly supervised semantic segmentation. In *Proceedings of the IEEE Conference on Computer Vision and Pattern Recognition*, pages 12275–12284, 2020.
- [35] Jifeng Dai, Kaiming He, and Jian Sun. Boxesup: Exploiting bounding boxes to supervise convolutional networks for semantic segmentation. In *Proceedings of the IEEE International Conference on Computer Vision*, pages 1635–1643, 2015.
- [36] Anna Khoreva, Rodrigo Benenson, Jan Hosang, Matthias Hein, and Bernt Schiele. Simple does it: Weakly supervised instance and semantic segmentation. In *Proceedings of the IEEE Conference on Computer Vision and Pattern Recognition*, pages 876–885, 2017.
- [37] Jonathan Long, Evan Shelhamer, and Trevor Darrell. Fully convolutional networks for semantic segmentation. In *Proceedings of the IEEE Conference on Computer Vision and Pattern Recognition*, pages 3431–3440, 2015.
- [38] Guolei Sun, Wenguan Wang, Jifeng Dai, and Luc Van Gool. Mining cross-image semantics for weakly supervised semantic segmentation. In *Proceedings of the European Conference on Computer Vision*, pages 347–365. Springer, 2020.
- [39] Peng-Tao Jiang, Ling-Hao Han, Qibin Hou, Ming-Ming Cheng, and Yunchao Wei. Online attention accumulation for weakly supervised semantic segmentation. *IEEE Transactions on Pattern Analysis and Machine Intelligence*, 2021.
- [40] Kunpeng Li, Yulun Zhang, Kai Li, Yuanyuan Li, and Yun Fu. Attention bridging network for knowledge transfer. In *Proceedings of the IEEE International Conference on Computer Vision*, pages 5198–5207, 2019.
- [41] Alexander Kolesnikov and Christoph H Lampert. Seed, expand and constrain: Three principles for weakly-supervised image segmentation. In *Proceedings of the European Conference on Computer Vision*, pages 695–711. Springer, 2016.
- [42] Wataru Shimoda and Keiji Yanai. Self-supervised difference detection for weakly-supervised semantic segmentation. In *Proceedings of the IEEE International Conference on Computer Vision*, pages 5208–5217, 2019.
- [43] Yu-Ting Chang, Qiaosong Wang, Wei-Chih Hung, Robinson Piramuthu, Yi-Hsuan Tsai, and Ming-Hsuan Yang. Weakly-supervised semantic segmentation via sub-category exploration. In *Proceedings of the IEEE Conference on Computer Vision and Pattern Recognition*, pages 8991–9000, 2020.